Journal of Photochemistry and Photobiology A: Chemistry 283 (2014) 38–44

Contents lists available at ScienceDirect

Journal of Photochemistry and Photobiology A: Chemistry

journal homepage: www.elsevier.com/locate/jphotochem

Synthesis of star poly(*N*-isopropylacrylamide) with end-group of zinc-porphyrin *via* ATRP and its photocatalytic activity under visible light

Nannan Qiu[a], Yanhui Li[a], Shuangli Han[c], Guihua Cui[a], Toshifumi Satoh[b], Toyoji Kakuchi[b], Qian Duan[a,*]

[a] *School of Materials Science and Engineering, Changchun University of Science and Technology, Changchun 130022, China*
[b] *Division of Biotechnology and Macromolecular Chemistry, Graduate School of Engineering, Hokkaido University, Sapporo 060-8628, Japan*
[c] *Changchun Institute of Optics, Fine Mechanics and Physics, Chinese Academy of Sciences, Changchun 130033, China*

ARTICLE INFO

Article history:
Received 19 November 2013
Received in revised form 23 February 2014
Accepted 14 March 2014
Available online 13 April 2014

Keywords:
Poly(*N*-isopropylacrylamide)
Zincporphyrin
Atom transfer radical polymerization
Photocatalyst

ABSTRACT

A series of well-defined star-shaped poly(*N*-isopropylacrylamide) (ZnTHPP-PAM) with zinc-porphyrin as the core was synthesized by atom transfer radical polymerization (ATRP). Zinc(II)meso-tetra(p-bromopropionylphenyl)porphyrin (ZnTHPP-Br) was employed as the initiator, and CuBr/tris(2-dimeoeth-yl)amine(Me_6TREN) was selected as the catalyst system. The structures of the target polymers were characterized by FT-IR and ^{1}H NMR. The polydispersity index (PDI) was obtained by gel permeation chromatography (GPC), indicating that the molecular weight distribution was narrow and the polymerization was well controlled. The lower critical solution temperatures (LCST) for the aqueous solutions of ZnTHPP-PAM were generated by using turbidimetry method. The result exhibited lower value as compared to that of NIPAM homopolymer, which was arose from the incorporation of the hydrophobic porphyrin core. The photocatalytic activity of ZnTHPP-PAM was verified by the degradation of Methylene Blue in the presence of hydrogen peroxide under visible light. It was worth noting that the catalytic efficiency was higher at the LCST of the polymer, which benefited to the reuse of the photocatalyst.

1. Introduction

Porphyrins are planar aromatic macrocycles consisting of four pyrrolic subunits linked by four methine bridges, which presents a delocalized 18π-electron aromatic cloud. And until now, porphyrins have been investigated extensively and used in a series of fields, including photosynthesis, photosensitization, oxidation, and electron transfer [1,2].

In the field of photocatalytic degradation, porphyrins and their derivatives are particularly promising due to their high electron transfer abilities and redox properties as well as the thermal and chemical stability [3]. And furthermore, porphyrins and metalloporphyrins can efficiently harvest sunlight and have high molar absorption coefficients in the visible region, high quantum yields of photo-excited triplet states. So, several free base porphyrins or metalloporphyrins have been reported to be powerful sensitizers for the photooxidation of phenols and naphthols in organic solvent system [4–11]. Unfortunately, these porphyrins are insoluble in aqueous solution and difficult to use as sensitizers to remove pollutants from wastewater.

In recent years, it is a topic of growing interest to photodegrade phenolic compounds using water-soluble porphyrin derivatives. The water-soluble porphyrin could show favorable catalytic efficiency because of all the catalytic activity can be effectively used. Some water soluble sulfophenyl porphyrin derivatives, such as iron complex of porphyrin have successfully used in the photodegradation of pollutants from wastewater [12,13]. However, its applications are restricted by the complexity and difficulty in separation recycling process from the reaction system after the catalytic degradation. It is easy to cause secondary pollution, if do not be handled properly. Thus, it is of great significance to develop a photocatalyst with efficient performance in the wastewater degradation system using water as medium, and could be recycled effectively in order to prevent secondary pollution.

Poly(*N*-isopropylacrylamide) (PNIPAM) has been the most frequently studied thermo sensitive polymer due to its lower critical

---

* Corresponding author. Tel.: +86 431 85583105; fax: +86 431 85583105.
E-mail address: duanqian88@hotmail.com (Q. Duan).

http://dx.doi.org/10.1016/j.jphotochem.2014.03.012

solution temperature (LCST) of 32 °C, which is close to the temperature of the human body [14–19]. Investigations on the phase transition of PNIPAM have revealed that its macromolecules processed dehydration and collapse from a hydrated, extended coil to a hydrophobic globule [20]. Functional PNIPAMs have been synthesized and employed in many fields, such as drug delivery systems, separation and purification, nanotechnology and bioengineering [21–26]. On the other hand, recently controlled/“living” radical polymerization (CRP) has been widely developed, which provides an efficient way of synthesizing polymers with designed structure and narrow molecular weight distribution. Atom transfer radical polymerization (ATRP), one of the most investigated CRP, could provide polymers with well-defined structure by using suitable initiators [27–32]. In the past few years, our group has synthesized several end-functionalized PNIPAMs *via* ATRP and the thermo-responsive properties were also studied [33–35]. However, to the best of our knowledge, there were few reports on the ATRP of *N*-isopropylacrylamide (NIPAM) with porphyrin derivatives as the initiator. In the present study, we attempt to immobilize the porphyrin onto the PNIPAM *via* ATRP, anticipate the improvements of the water-solubility and thermo responsive property of porphyrin for further applications in catalyst recycling by simple heating and filtration.

Herein, the “core-first” star polymer ZnTHPP-PAM with porphyrin as the core and PNIPAM as the arms was synthesized *via* ATRP. The photocatalytic activity was investigated on the oxidative degradation of Methylene Blue under the visible light irradiation and the recycling experiments were conducted. The results showed that the polymer with low polydispersity possessed both thermo-responsive property and photocatalytic activity which could be recycled conveniently after the catalytic process. The polymer was demonstrated to be a robust functional catalyst for the photodegradation of dyes.

2. Experimental

2.1. Materials

N-isopropylacrylamide (99%, Aldrich) was recrystallized twice from benzene/hexane (10:1, v/v) prior to use. 2-bromopropionyl bromide (99%, Acros), Copper(I) bromide (CuBr, 99%, Aldrich) were available commercially and used without further purification. Tris(2-(dimethylamino)ethyl)amine (Me_6TREN) was synthesized according to the literature [36]. All other chemicals were purchased from Sinopharm Chemical Reagent Co. and were used as received.

2.2. Characterization

^1H NMR spectra were carried out on a Bruker Avance 400 MHz spectrometer at ambient temperature, using $CDCl_3$ or DMSO-d_6 as solvent, TMS for ^1H calibration. Element analysis was obtained on a Carlo Erba-MOD1106 instrument. Fourier transform infrared (FT-IR) spectra were recorded on a FTIR 8400S (Shimadzu) spectrometer. The spectra were collected at 40 scans with a resolution of 4 cm^{-1}. Molecular weights ($M_{n,GPC}$) and polydispersity (M_w/M_n) were measured on a gel permeation chromatograph (GPC) using a Waters e2695 separations module, two waters styragel columns (HR4 and HT3, 300 mm × 7.8 mm, 5 μm particles; exclusion limits: 5000–30,000 and 500–30,000 g mol^{-1}, respectively) and a Waters 2414 refractive index dector maintained at 35 °C, the polymer molar masses were determined using linear polystyrene as calibration standards, THF was used as a mobile phase at a flow rate of 1.0 mL/min. Ultraviolet–visible (UV–vis) spectra were measured on a UV mini 1240 (Shimadzu) spectrophotometer.

2.3. Synthesis of 5,10,15,20-tetra(4-(2-bromopropoxy)phenyl)-21H,23H-zinc porphyrin (ZnTHPP-Br)

The synthesis of 5,10,15,20-tetra(4-hydroxyphenyl)-21H,23H-porphine(THPP) and 5,10,15,20-tetra(p-hydroxyphenyl)-21H, 23H-zincporphyrin(Zn-THPP) was depicted in Scheme S1 and Scheme S2.

ZnTHPP-Br was synthesized as follows (Scheme 1): ZnTHPP (300 mg, 4.05×10^{-4} mol), triethylamine (2×10^{-3} mol, 1.13 mL) and a mixed solution of ethyl ether and dichloromethane (100 mL, 1:1 v/v) were mixed under nitrogen in an ice bath. 2-Bromopropionyl bromide (2×10^{-3} mol, 0.83 mL) in dichloromethane (10 mL) was added dropwise over 15 min. The mixture was allowed to warm to room temperature and then stirred for 24 h. The reaction mixture was then washed with deionized water three times, and the organic layer was reduced to a minimum under vacuum. The resulting solution was purified by silica flash chromatography [SiO_2, petroleum dichloromethane/methanol (200:1 v/v) as the eluent]. After the removal of solvent, the porphyrin was isolated as a purple powder.

FT-IR (KBr, cm^{-1}): 2851–2964 cm^{-1} ($\nu_{-CH_2,\ -CH_3}$), 1762 cm^{-1} ($\nu_{C=O}$), 729 cm^{-1}, 810 cm^{-1}, 990 cm^{-1} are the skeletal vibration of pyrrole [Fig. S3(A)]. ^1H NMR (δ, DMSO-d_6, ppm): 8.82 (s, 8H, pyrrole—H), 8.25 (d, 8H, Ar—OH), 7.62 (d, 8H, Ar—H), 5.2 (q, 4H, —CH—), 1.87 (d, 12H, —CH_3) [Fig. S4(A)]. Anal. Calcd for $C_{58}H_{46}Br_4N_4O_8Zn$: C, 53.10; H, 3.53; N, 4.27. Found: C, 53.05; H, 3.59; N, 4.28.

2.4. Synthesis of star-shaped poly(N-isopropylacrylamide) with ZnTHPP-Br as the core (ZnTHPP-PAM)

A general procedure employed for the preparation of ZnTHPP-PAM was as follows (Scheme 1): after deoxygenated by bubbling with nitrogen, NIPAM (224 mg, 2.00 mmol), CuBr (15.84 mg, 0.08 mmol), and Me_6TREN (19.2 μL, 0.08 mmol) were dissolved in 2 mL of DMF/water (2:1, v/v), followed by degassing *via* three freeze-pump-thaw cycles. Deoxygenated solution of ZnTHPP-Br (12.8 mg, 0.01 mmol) in DMF (0.5 mL) was then added into the reaction flask for further polymerization. The reaction was carried out for 12 h at 60 °C under a nitrogen atmosphere. Polymerization was terminated by exposing to air. Then the reaction mixture was diluted with THF and passed through an alumina column. The resulting polymer was purified by dialysis using a cellophane tube (MWCO, 2000) in DMF. After removing the solvents, the residue was dried in *vacuo* for 24 h to give the pure ZnTHPP-PAM.

FT-IR (KBr, cm^{-1}): 3315 cm^{-1} (ν_{N-H}), 2876–2972 cm^{-1} ($\nu_{-CH_2,\ -CH_3}$), 1650 cm^{-1} ($\nu_{C=O}$), 1540 cm^{-1}(δ_{N-H}) [Fig. 3S(B)]. ^1H NMR (δ, DMSO-d6, ppm): 8.92(s, 8H, pyrrole—H), 8.34(d, 8H, Ar—OH), 7.82(d, 8H, Ar—H), 6.40 (51H, p—NH), 4.00 (51H, P—CH—), 2.24 (51H, P—CH′—),1.56(102H, P—CH_2—), 1.23(300H, P—CH_3) [Fig. S4(B)].

2.5. Cloud points measurement

Cloud points (CP) of the aqueous solution of ZnTHPP-PAM were measured by UV–vis spectroscopy. The sample dissolved in water (2 mg/mL) was poured into a thermally controlled cell (1 cm × 1 cm). Transmittance of the aqueous solution at 500 nm was monitored with heating rate of 0.5 °C/min.

2.6. Photocatalytic degradation test

Catalytic oxidation of Methylene Blue was carried out in the aqueous solution at room temperature using hydrogen peroxide (H_2O_2) as the oxidant under the visible light irradiation [a 500 W

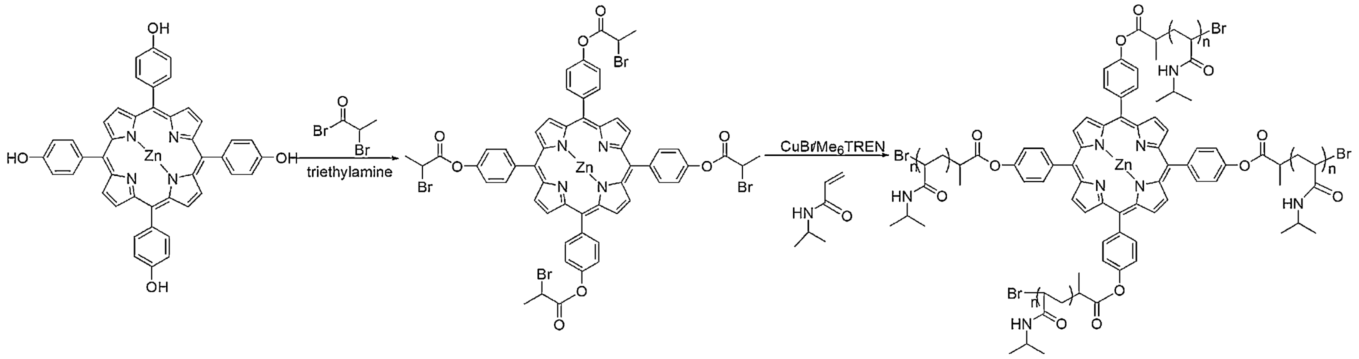

Scheme 1. Synthesis route of ZnTHPP-PAM.

Halogen lamp through a glass filter (λ > 400 nm) was used as an illuminant]. The light source (halogen lamp) is the full spectrum, we used glass filter to cut off the light of λ > 400 nm and guarantee irradiation with visible light. The pH value of the solution was adjusted by adding standard buffer solutions. The initial concentration of Methylene Blue solution was 4×10^{-5} mol/L. After the polymeric catalyst ZnTHPP-PAM ($M_{n,GPC}$ = 8300, M_w/M_n = 1.18) was added into Methylene Blue solution under stirring, the samples (3 mL) were monitored immediately at given time intervals on a UV–vis spectrometer.

Table 1
λ_{max} of the B-band and Q-Bands above for THPP, Zn-THPP, ZnTHPP-Br and ZnTHPP-PAM (CH_2Cl_2, 0.4 mol/L).

	λ_{max}				
	B-band	Q-band			
THPP	415	518	556	596	652
Zn-THPP	415		549	589	
ZnTHPP-Br	415		549	589	
ZnTHPP-PAM[a]	422		560	604	

[a] M_n = 8300, M_w/M_n = 1.22.

3. Results and discussion

3.1. Synthesis and characterization

Well-defined star-shaped poly(*N*-isopropylacrylamide) with zinc-porphyrin core (ZnTHPP-PAM) was successfully prepared *via* ATRP, by using ZnTHPP-Br as the initiator, CuBr/Me_6TREN as the catalyst system for 12 h at 60 °C. After purification, the structure of target polymer was characterized by ^{1}H NMR, GPC, and Fourier transform infrared (FT-IR) techniques. The occurrence of the ATRP reaction between the ZnTHPP-Br and *N*-isopropylacrylamide could be confirmed. Fig. S3(B) showed the IR spectra of ZnTHPP-PAM. The characteristic absorptions of PNIPAM could be clearly observed, as evidenced by the presence of a carbonyl stretching vibration ($\upsilon_{C=O}$) at 1650 cm^{-1} and the N—H bending vibration (δ_{N-H}) at 1550 cm^{-1}. The strong absorbance at 3304 cm^{-1} was assigned to the stretching vibration (υ_{N-H}) of acylamino group.

Although the characteristic peaks of the porphyrin skeleton could not be resolved clearly in FT-IR spectra, the structure was further confirmed by ^{1}H NMR and UV–vis spectra. Fig. S4(B) showed the ^{1}H NMR spectra of ZnTHPP-PAM. The signals at 6.51, 4.22, 2.28, 1.64 and 1.35 ppm assigned to the protons on the repeated units of NIPAM could be clearly observed. Moreover, the signals at 8.85, 8.22, 7.64 ppm were attributed to the protons on the porphyrin core. The results suggested that the star-shaped ZnTHPP-PAM with porphyrin as the core was successfully prepared *via* ATRP. The molecular weight could be also obtained by comparing the resonance signals for the aromatic part of the porphyrin group with those of the methine protons on PNIPAM. The molecular weight of ZnTHPP-PAM ($M_{n,GPC}$ = 8300) determined by the ^{1}H NMR analysis was 8600, which was relatively higher than that determined by the GPC analysis. The probable reason was that the hydrodynamic volume of star-shaped polymer was somewhat smaller relative to that of the linear analog with the same molecular mass.

The UV–vis spectra of THPP exhibited a strong Soret band and four Q-bands as shown in Fig. 1(A). The Q-band peaks of ZnTHPP reduced to two, which were accorded with those observed for similar porphyrin metal complexes [37]. Meanwhile, the UV–vis absorptions of ZnTHPP-PAM showed the bathochromic shifts as compared to those of ZnTHPP-Br, it is because that a change of polarity around Zn-porphyrin by polymer chains which is attributed to a shift of absorption band. The maximum absorption wavelengths (λ_{max}) were showed in Table 1. In addition, it was well known that most of the porphyrins exhibited poor water

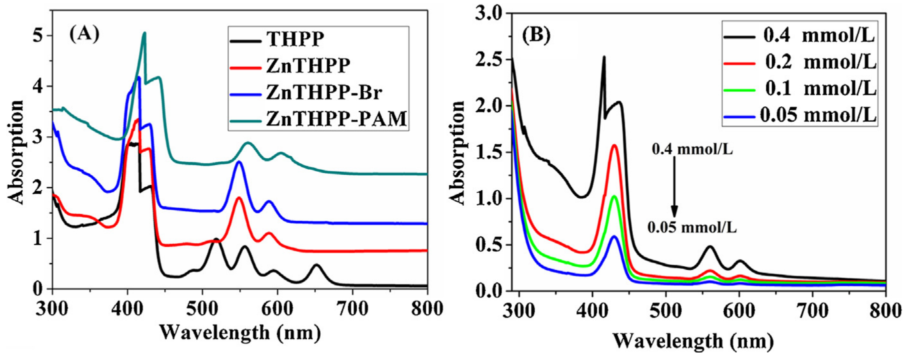

Fig. 1. (A) UV–vis spectra of THPP, ZnTHPP, ZnTHPP-Br and ZnTHPP-PAM in CH_2Cl_2 (0.4 mmol/L) and (B) UV–vis spectra of ZnTHPP-PAM in aqueous solution with different concentrations.

Table 2
Data of the polymerization reactions and LCST of ZnTHPP-PAM samples.

Run	$[M]_0/[I]_0$	Con.[a] (%)	M_n [b]	M_w [b]	M_w/M_n	LCST[c] (°C)	Q.S.[d] (mg/100 mg)
1	300	73	13,100	16,100	1.23	31.2	23
2	250	50	10,300	12,400	1.20	29.7	18
3	200	42	8300	9800	1.18	29.3	13.2
4	150	37	6200	7100	1.14	29.0	8.5
5	100	15	4100	4400	1.07	28.9	4.7

[a] Determined by gravimetric measurement.
[b] Determined by GPC using THF as eluent relative to polystyrene standards.
[c] Measured by turbidimetry using UV–vis spectrophotometer.
[d] Measured by balancing method at room temperature.

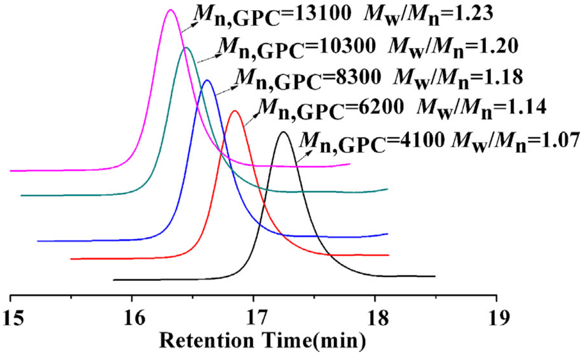

Fig. 2. GPC traces of ZnTHPP-PAM.

solubility which restricted their applications for photocatalytic degradation. In the present study, the water solubility of ZnTHPP-PAM was improved. The target polymer could dissolve in water and common organic solvents. It could be seen from the UV–vis spectra of ZnTHPP-PAM in aqueous solution with different concentrations Fig. 1(B). The UV–vis absorptions of the samples with the concentrations of ZnTHPP-PAM grown from 0.05 to 0.4 mmol/L showed invariant patterns except the enhanced absorbance of the Soret band and Q-bands. Meanwhile the quantitative solubility of ZnTHPP-PAMs for water is measured. The results are showed in Table 2, it is clearly seen that the quantitative solubility of ZnTHPP-PAM continue to improve with the increase of molecular weight. From the above, it could be concluded that the ZnTHPP-PAM exhibited good solubility and stability in water no less articulate than of other water-soluble porphyrin compounds [38].

The M_n values of the ZnTHPP-PAM were determined by GPC using polystyrene as the standard. The results were presented in Table 2. GPC traces of ZnTHPP-PAM (Fig. 2) were relatively symmetric and showed no tailing at either side. It suggested the absence of any small molecule residues, such as the initiator, monomer or other byproducts, in the final product. Moreover, the polymers showed narrow molecular weight distributions in the range of 1.07–1.23, which demonstrated that the polymerizations were performed in a controlled process.

3.2. Thermoresponsive property of ZnTHPP-PAM

In order to study the thermoresponsive property of ZnTHPP-PAM, we measured the CP of ZnTHPP-PAM by UV–vis spectroscopy, the result showed in Fig. 3: when the temperature was lower than LCST, ZnTHPP-PAM exhibited good solubility in water. Whereas, the macromolecules processed dehydration and collapse from a hydrated, extended coil to a hydrophobic globule, so the solution emerged turbid phenomenon gradually when the temperature became higher than LCST.

A sharp transition was obviously observed in the CP curve as shown in Fig. 3, indicating the thermo-responsive properties of ZnTHPP-PAM. In the present study, the LCST was arbitrarily defined as the temperature corresponding to a 10% decrease of the transmittance at 500 nm [39,40]. The LCSTs of the aqueous solutions of ZnTHPP-PAM were listed in Table 2. The values were lower than that of NIPAM homopolymer owing to the incorporation of hydrophobic porphyrin groups. This phenomenon was consistent with the result that the hydrophobic groups decreased the thermal phase transition temperature of PNIPAM as previously reported [41,42]. In addition, the LCST values of the ZnTHPP-PAM samples gradually approached to *ca.* 32 °C with the molecular weight increasing. It was attributed to the weaker effect of the porphyrin core on the performance of polymer, arising from the lowered proportion of porphyrin core in the polymer chain upon the increasing of molecular weight.

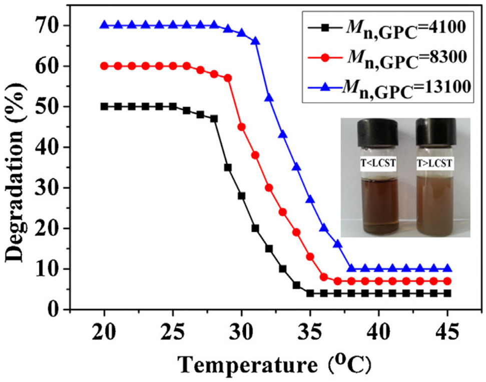

Fig. 3. Temperature dependence of optical transmittance at wavelength of 500 nm obtained for aqueous solutions of ZnTHPP-PAM (2 mg/mL).

3.3. Photocatalytic activity of ZnTHPP-PAM on Methylene Blue

The mechanism for catalytic degradation of metalloporphyrin imitating catalase was shown in Fig. 4. Hydrogen peroxide acted as the oxidant in the process of photo catalytic degradation. Firstly, hydrogen peroxide generated OOH^- by the heterolysis. Secondly,

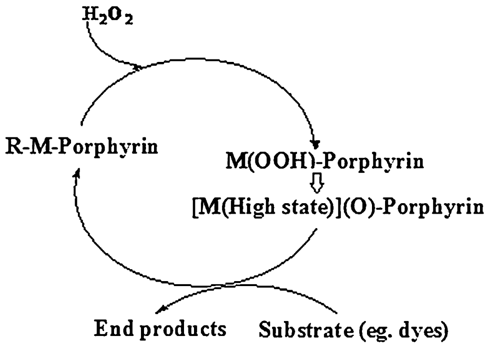

Fig. 4. The mechanism of catalytic degradation of metallophthalocyanine imitating catalase.

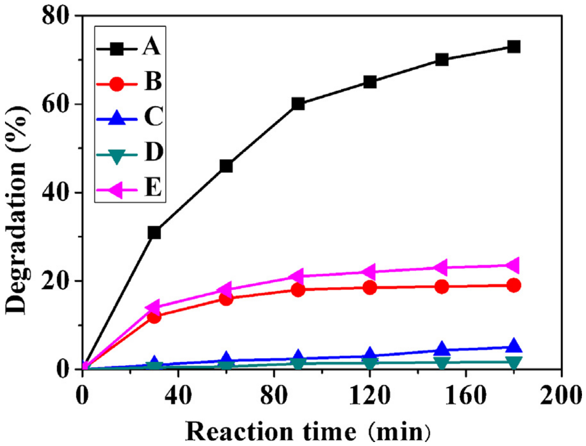

Fig. 5. Kinetic curves of the photocatalytic degradation of Methylene Blue under various different conditions at 29 °C: A ZnTHPP-PAM + H_2O_2 + visible light; B H_2O_2 + visible light; C: ZnTHPP-PAM + H_2O_2; D: ZnTHPP-PAM + visible light; E: ZnTHPP + H_2O_2 + visible light. Experimental condition: [Methylene Blue] = 4×10^{-5} mol/L, [ZnTHPP-PAM (M_n = 8300)] = 2×10^{-5} mol/L, [H_2O_2] = 40 mL/L, pH 2, $\lambda > 450$ nm.

an axial coordination of OOH^- to the metal ion of metalloporphyrin occurred. Finally the generated complexes transformed into high metal oxygen complexes by further heterolysis, and the high metal oxygen complexes oxidative degraded organic dyes [43–46].

Herein, Methylene Blue, a kind of commercial non-biodegradable toxic dye with aromatic structure, was selected as the substrate to investigate the catalytic performance of ZnTHPP-PAM under visible light irradiation. The degradation of Methylene Blue in aqueous solution was estimated by the changes of the absorption intensity at the maximum absorption wavelength (around 650 nm). The degradation rate (D) could be defined as the ratio of the absorbance decrement to the initial intensity of Methylene Blue aqueous solution (as described in the following equation):

$$D = \frac{A_0 - A}{A_0} \times 100\%$$

where A_0 was the initial absorption intensity at the maximum absorption wavelength, and A was the absorption intensity at any time during the measurement.

Although the catalytic degradation of organic pollutants using H_2O_2 as the oxidant and metalloporphyrin as the photocatalyst was investigated detailedly in previous works [47], it was necessary to carry out further controlled experiments of the degradation for Methylene Blue to confirm the catalytic activity of the polymer (ZnTHPP-PAM). The results were shown in Fig. 5. It was clearly seen that Methylene Blue was hardly degraded in the presence of ZnTHPP-PAM under visible light (curve D), and the semblable phenomenon was observed in the presence of ZnTHPP-PAM and H_2O_2 without the light irradiation (curve C). Meanwhile, in the presence of only H_2O_2 under the visible light the degradation of Methylene Blue was mere 10% (curve B) and in the case of ZnTHPP + H_2O_2 + visible light (curve E) the degradation rate showed a little more increased value (20%) relative to that as indicated by curve B. From the above phenomenon, it could be concluded that ZnTHPP showed a weak photocatalytic property, due to the suspending of ZnTHPP in the catalytic systems resulted from the bad solubility. On the other hand, more than 75% of Methylene Blue was degraded by H_2O_2 under visible light in the presence of ZnTHPP-PAM after 150 min irradiation (curve A). The results clarified that the strong coactive ZnTHPP-PAM + H_2O_2 + visible light system was essential for the degradation of Methylene Blue. The immobilizing of the porphyrin onto PNIPAM increased the water solubility of the photocatalyst, resulting in the whole photocatalytic degradation process in the homogeneous system with greatly improved catalytic efficiency.

In order to get an insight into the relationship between the degradation rate and pH-values, the experiments of photocatalytic degradation under various different pH values with consistent other conditions were preformed (as shown in Fig. 6(A)). Indeed, the increase of pH value is benefit for the generation OOH—, so the degradation rate gradually increased with pH increasing in the beginning stage. When pH was 2 the degradative rate could reach 87% due to the increased concentration of OOH^- arising from the enhancement of ionization. Whereas, the degradation rate showed a gradually declined tendency along with the further increase of pH value. As a result, the degradation rate was only 15% while the pH was 8. The probable reasons include two point: firstly, in addition to generating the complexes [M(OOH)-porphyrin], there is a part of the superfluous OOH^- as the growing of the concentration of OOH^- with pH increasing, and the superfluous OOH^- may lead to an further axial coordination to M(OOH)-porphyrin competing with dye molecules which reduce the chances of the dye molecules combining with [M(OOH)-porphyrin]. Secondly, the different relative equilibrium concentrations of the monomer of the porphyrin and its dimer at different pHs, with the monomer being favored at acidic pH and the dimer predominates at basic pH. The dimer of the porphyrin has lower catalytic activity to be occupied, resulting in the decline of the degradation rate [48]. From Fig. 6(A), we also observed a modest rebound in the degradation rate among the pH value of 9–12 because of the reaction between the dye molecules and hydroxyl ions (OH—) which leads to the generation of the intermediates, and these intermediates are easy to degrade.

Considering the polymeric catalyst exhibited the thermo-responsive property, the effect of temperature on the oxidative degradation of Methylene Blue was investigated. Fig. 6(B) showed the experimental results. The degradation rate of Methylene Blue processed few variations below 29 °C while the reaction system of photocatalytic degradation remained homogeneous phase. The degradation rate evidently went up with the further increase of temperature and reached the peak value of 47% at 29 °C. The temperature of turning point was slightly lower than the LCST of ZnTHPP-PAM. The interesting phenomenon was similar to the study on the photocatalytic degradation of 2-mercaptoethanol by Co-TACAPc/NIPAM copolymer reported by Chen [49,50]. When the system temperature approached the LCST of ZnTHPP-PAM, the polymer chain turned to tightly packed globules from random coils to form a micelle-like structure. In the micelle-like area, the concentration of the active center was relatively higher, so the degradation rate increased significantly. The other probable reason is that Methylene Blue and hydrogen peroxide may be encapsulated into the quasi-micelles during this transition, so the distance between Methylene Blue and hydrogen peroxide was diminished which is beneficial to promote the axial coordination of the oxidant H_2O_2 and the center metal atom Zn. In order to test this phenomenon, we did a series of contrast experiments, the result showed in Fig. S5: we can see that the strength of the ultraviolet absorption declines significantly when the temperature rises from 20 °C to 29 °C. For purpose of avoiding the interfering from the interaction between Methylene blue and hydrogen peroxide, we did not add hydrogen peroxide in whole experiment process. The experimental results could show evidence about the encapsulation of ZnTHPP-PAM for small molecules. Furthermore, Poly(*N*-isopropylacrylamide) (PNIPAM) has been used in drug delivery systems frequently, which may prove the encapsulation of ZnTHPP-PAM in some ways. However, the degradation rate gradually declined along with the further temperature rising. It was because that ZnTHPP-PAM precipitated from the aqueous solution when the temperature exceeded the LCST. The system became heterogeneous and the center zinc of

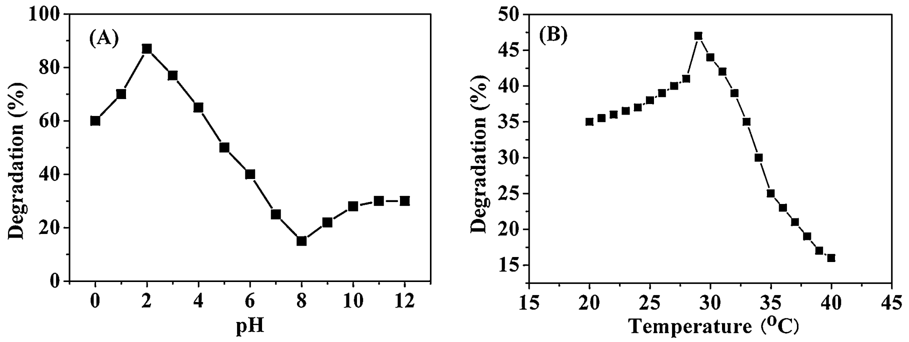

Fig. 6. Degradation of Methylene Blue under different pH-values conditions after 210 min at 29 °C (A) and effect of temperature on the degradation of Methylene Blue within 60 min at pH 2 (B). Other experimental condition: [Methylene Blue] = 4 × 10^{-5} mol/L, [ZnTHPP-PAM (M_n = 8300)] = 2 × 10^{-5} mol/L, [H_2O_2] = 40 mL/L, λ > 450 nm.

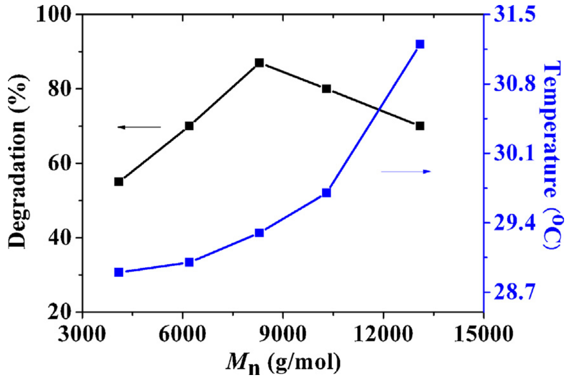

Fig. 7. Degradation of Methylene Blue under different molecular weight after 3 h at LCST of polymers. Other experimental condition: [Methylene Blue] = 4 × 10^{-5} mol/L, [ZnTHPP-PAM] = 2 × 10^{-5} mol/L, [H_2O_2] = 40 mL/L, λ > 450 nm.

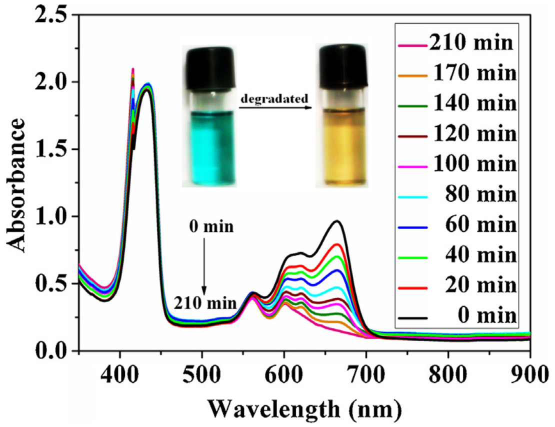

Fig. 8. UV–vis spectral changes of Methylene Blue in aqueous solution (initial concentration: 4 × 10^{-5} mol/L) as a function of irradiation time. [ZnTHPP-PAM (M_n = 8300)] = 2 × 10^{-5} mol/L, [H_2O_2] = 40 mL/L, pH 2, λ > 450 nm.

porphyrin was embedded by the PNIPAM chains which hindered the axial coordination.

The polymers (ZnTHPP-PAM) with different molecular weights were prepared and the weight effect on the degradation rate was also studied. From the above discussions, it was demonstrated that the polymeric catalyst showed the highest catalytic efficiency under the temperature slightly lower than the corresponding LCST. So the temperature of the following photocatalytic experiments was maintained at LCST, and the results were shown in Fig. 7. The degradation rate exhibited a sharply rising trend with the gradual increase of the molecular weight, and reached about 90% when the molecular weight was 8300. The phenomenon could be explained from two aspects. Firstly, the molecular weight increasing resulted in the rising temperature of photocatalytic system, which intensified the molecular motion and facilitated the oxidative degradation of Methylene Blue. Secondly, the longer antennas of the polymer and larger molecular weight benefited the encapsulation of Methylene Blue and hydrogen peroxide in quasi-micelles, and caused the improved efficiency of degradation. However, when the molecular weight reached 10,300 and 13,100, the degradation rate relatively decreased. It is because that the excessively longer antennas embedded the active center zinc porphyrin or Methylene Blue and hydrogen peroxide are encapsulated by the PNIPAM chains which hindered the axial coordination between H_2O_2 and the metal atom Zn.

Based on the above discussions, we summarized the best experimental conditions. Fig. 8 showed the UV–vis spectral variations of Methylene Blue as a function of irradiation time. It could be seen that the concentration of Methylene Blue gradually declined along with increasing reaction time in the Methylene Blue/ZnTHPP-PAM/H_2O_2 photocatalytic system. Methylene Blue absorption peaks at around 650 nm and the characteristic absorption bands decreased rapidly and disappeared after the degradation of 210 min. Concomitantly, the color of the reaction solution changed from the initially blue to light transparent as shown in Fig. 8. In addition, the characteristic absorption peaks of ZnTHPP-PAM at 430 nm were almost invariable with the increasing reaction time, suggesting the polymeric catalyst was relatively stable during the photodegradation of Methylene Blue.

In order to avoid secondary pollution to the environment, excellent catalyst should have the advantages of recycling. So a series of recycling experiments were performed for the degradation of Methylene Blue by the polymeric catalyst. In each run, a fresh

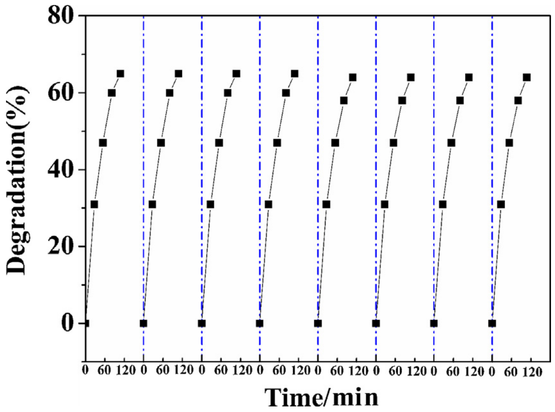

Fig. 9. Recycling experiments for degradation of Methylene Blue aqueous solution under visible light (λ > 450 nm). [Methylene Blue] = 4 × 10^{-5}mol/L, [ZnTHPP-PAM (M_n = 8300)] = 2 × 10^{-5} mol/L, [H_2O_2] = 40 mL/L, pH 2.

solution of Methylene Blue was supplied for maintenance of its initial concentration. At the end of each run, the thermo-responsive catalyst was separated by elevating the temperature of the reaction system and dried under vacuum without further treatment. The catalytic activity was nearly unchanged in the reaction runs as shown in Fig. 9. It suggested that the polymeric catalyst had a good stability during the recycling experiments and the thermosensitive catalyst could be reused from the reaction system through a simple operation.

4. Conclusions

A novel star-shaped polymer with zinc porphyrin as the core and PNIPAM as the antennas was prepared *via* ATRP. Then, the PDI indicated that the molecular weight distribution was narrow and the polymerization was well controlled. However, the LCSTs of ZnTHPP-PAM decreased owing to the incorporation of the zinc porphyrin core. The catalytic properties of ZnTHPP-PAM were investigated for the oxidative degradation of Methylene Blue in aqueous medium, and the results showed that the polymeric catalyst was highly effective for the oxidative degradation of Methylene Blue around its LCST and the catalytic activity was nearly unchanged in the recycling experiments without any significant loss after the uncomplicated recovery processing. Therefore, the polymeric catalyst was demonstrated to be a robust functional catalyst for the photodegradation of dyes.

Acknowledgements

We are grateful to Jilin Science & Technology Department (20070556, 20140204017GX), Science and Technology Bureau of Changchun City project (2008280, 2013060) Foundation for Strategical Research for financial support.

Appendix A. Supplementary data

Supplementary data associated with this article can be found, in the online version, at http://dx.doi.org/10.1016/j.jphotochem.2014.03.012.

References

[1] K.M. Kadish, K.M.R Smith, Guilard, the Porphyrin Handbook: Inorganic Organometallic and Coordination Chemistry, Elsevier, New York, 2000.
[2] L. Tasseroula, S.D. Lamberta, D. Eskenazia, M. Amouraa, C.A. Páeza, S. Hiligsmannb, P. Thonartb, B. Heinrichs, J. Photochem. Photobiol. A 272 (2013) 90–99.
[3] V. Hequet, P. Le Cloirec, C. Gonzalez, B. Meunierc, Chemosphere 41 (2000) 379–384.
[4] M. Fukushima, M. Kawasaki, A. Sawada, H. Ichikawa, K. Morimoto, K. Tatsumi, S. Tanaka, J. Mol. Catal. A: Chem. 187 (2002) 201–205.
[5] D. Murtinho, M. Pineiro, M.M. Pereira, A.M.D. Gonsalves, L.G. Arnaut, M.D. Miguel, H.D. Burrows, J. Chem. Soc. Perkin Trans. 2 (2000) 2441–2447.
[6] M. Fukushima, K. Tatsumi, Environ. Sci. Technol. 39 (2005) 9337–9341.
[7] G. Lente, J.H. Espenson, Green Chem. 7 (2005) 28–32.
[8] M. Fukushima, K. Tatsumi, J. Hazard. Mater. 144 (2007) 222–227.
[9] D. Smejkalova, A. Piccolo, Environ. Sci. Technol. 40 (2006) 1644–1649.
[10] M. Moghadama, S. Tangestaninejad, V. Mirkhani, I. Mohammadpour-Baltork, R. Shaibani, J. Mol. Catal. A: Chem. 219 (2004) 73–78.
[11] G. Mele, R. Del Sole, G. Vasapollo, E. Garcia-Lopez, L. Palmisano, M. Schiavello, J. Catal. 217 (2003) 334–337.
[12] E. Silva, M.M. Pereira, H.D. Burrows, M.E. Azenha, M. Sarakha, M. Bolte, Photochem. Photobiol. Sci. 3 (2004) 200–204.
[13] C.J.P. Monteiro, M.M. Pereira, M.E. Azenha, H.D. Burrows, C. Serpa, L.G. Arnaut, M.J. Tapia, M. Sarakha, P. Wong-Wah-Chung, S. Navaratnam, Photochem. Photobiol. Sci. 4 (2005) 617–621.
[14] X.Y. Shen, W.Y. Lu, G.H. Feng, Y.Y. Yao, W.X. Chen, J. Mol. Catal. A: Chem. 298 (2009) 17–22.
[15] Z.G. Xiong, Y.M. Xu, Chem. Mater. 19 (2007) 1452–1458.
[16] P. Zhao, J.W. Woo, Y.S. Park, Y.N. Song, F.S. Zhang, Macromol. Res. 18 (2010) 496–501.
[17] B. Agboola, K.I. Ozoemena, T. Nyokong, J. Mol. Catal. A: Chem. 248 (2006) 84–92.
[18] E.S. Gil, S.M. Hudson, Prog. Polym. Sci. 29 (2004) 1173–1222.
[19] H.G. Schild, Prog. Polym. Sci. 17 (1992) 163–249.
[20] A. Yamazaki, J.M. Song, F.M. Winnik, J.L. Brash, Macromolecules 31 (1998) 109–115.
[21] I. Ankareddi, C.S. Brazel, Int. J. Pharm. 336 (2007) 241–247.
[22] K. Fujimoto, C. Iwasaki, C. Arai, M. Kuwako, E. Yasugi, Biomacromolecules 1 (2000) 515–518.
[23] X.Z. Zhang, R.X. Zhuo, J.Z. Cui, J.T. Zhang, Int. J. Pharm. 235 (2002) 43–51.
[24] T. Matsuda, Y. Saito, K. Shoda, Biomacromolecules 8 (2007) 2345–2349.
[25] S.S. Pennadam, M.D. Lavigne, C.F. Dutta, K. Firman, D. Mernagh, D.C. Górecki, C. Alexander, J. Am. Chem. Soc. 126 (2004) 13208–13209.
[26] X.J. Lu, L.F. Zhang, L.Z. Meng, Y.H. Liu, Polym. Bull. 59 (2007) 195–206.
[27] J.S. Wang, K. Matyjaszewski, J. Am. Chem. Soc. 117 (1995) 5614–5615.
[28] M. Kato, M. Kamigaito, M. Sawamoto, T. Higashimura, Macromolecules 28 (1995) 1721–1723.
[29] K. Matyjaszewski, J.H. Xia, Chem. Rev. 101 (2001) 2921–2990.
[30] G. Masci, L. Giacomelli, V. Crescenzi, Macromol. Rapid Commun. 25 (2004) 559–564.
[31] W. Jakubowski, K. Matyjaszewski, Angew. Chem. Int. Ed. 45 (2006) 4482–4486.
[32] M. Kimura, H. Ueki, K. Ohta, K. Hanabusa, H. Shirai, N. Kobayashi, Chem. Eur. J. 10 (2004) 4954–4959.
[33] Q. Duan, A. Narumi, Y. Miura, X.D. Shen, S.I. Sato, T. Satohand, T. Kakuchi, Polym. J. 38 (2006) 306–310.
[34] X.D. Tao, Z.G. Gao, T. Satoh, Y. Cui, T. Kakuchi, Q. Duan, Polym. Chem. 2 (2011) 2068–2071.
[35] Z.G. Gao, X.D. Tao, Y. Cui, T. Satoh, T. Kakuchi, Q. Duan, Polym. Chem. 2 (2011) 2590–2596.
[36] M. Ciampolini, N. Nardi, Inorg. Chem. 5 (1966) 41–44.
[37] D.B. Papkovsky, T.C. O'riordan, J. Fluoresc. 15 (2005) 569–584.
[38] J.H. Caia, J.W. Huang, P. Zhao, Y.H. Zhou, H.C. Yua, L. Nian, J. Mol. Catal. A: Chem. 292 (2008) 49–53.
[39] S.T. Lin, K. Fuchise, Y.G. Chen, R. Sakai, T. Satoh, T. Kakuchi, W.C. Chen, Soft Matter 5 (2009) 3761–3770.
[40] Q. Duan, Y. Miura, A. Narumi, X.D. Shen, S.I. Sato, T. Satoh, T. Kakuchi, J. Polym. Sci. A: Polym. Chem. 44 (2006) 1117–1124.
[41] Y. Xia, X.C. Yin, N.A.D. Burke, H.D.H. Stover, Macromolecules 38 (2005) 5937–5943.
[42] Y. Xia, N.A.D. Burke, H.D.H. Stover, Macromolecules 39 (2006) 2275–2283.
[43] D. Dolphin, T.G. Traylor, L.Y. Xie, Acc. Chem. Res. 30 (1997) 251–259.
[44] B. Meunier, Chem. Rev. 92 (1882) 1411–1456.
[45] R. Neumann, M. Gara, J. Am. Chem. Soc. 116 (1994) 5509–5510.
[46] D. Keilin, E.F. Hartree, Biochemistry 39 (1945) 293–301.
[47] W. Nam, S.Y. Oh, Y.J. Sun, J. Kim, W.K. Kim, S.K. Woo, W. Shin, J. Org. Chem. 68 (2003) 379–386.
[48] R. Su, J. Sun, Y.P. Sun, K.J. Deng, D.M. Cha, D.Y. Wang, Chemosphere 77 (2009) 1146–1151.
[49] W.X. Chen, B.Y. Zhao, Y. Pan, Y.Y. Yao, S.S. Lu, S.L. Chen, L.J. Du, J. Colloid Interface Sci. 300 (2006) 626–632.
[50] W.X. Chen, W.Y. Lü, X.Y. Shen, Y.Y. Yao, Sci. China Chem. 53 (2010) 638–644.